

Grid Connected Current Controlled Boost Inverter Based Battery Supported Fuel Cell

Kalyan Chakravarthy Palagiri

M.Tech Student Scholar,

Department of Electrical & Electronics Engineering,
Thandra Paparaya Institute of Science & Technology,
Bobbili; Vizianagaram (Dt); A.P, India.

Dasari Uma Maheswara Rao

Assistant Professor,

Department of Electrical & Electronics Engineering,
Thandra Paparaya Institute of Science & Technology,
Bobbili; Vizianagaram (Dt); A.P, India.

Abstract :

This paper, proposes an analysis and design of a high efficiency boost-inverter with battery storage in fuel cell. When low-voltage unregulated fuel cell (FC) output is conditioned to generate AC power, two stages are required. The boost-inverter topology that achieves both boosting and inversion functions in a single-stage is used to develop an FC-based energy system which offers high conversion efficiency, low-cost and compactness. The low-frequency current ripple is supplied by the battery which minimizes the effects of such ripple being drawn directly from the FC itself. Moreover, this system can operate either in a grid-connected or stand-alone mode. In the grid-connected mode, the boost-inverter is able to control the active (P) and reactive (Q) power using an algorithm based on a Second Order Generalized Integrator (SOGI) which provides a fast signal conditioning for single phase systems.

Index Terms:

Fuel cell (FC) power conditioning system, three-phase boost-inverter.

I. INTRODUCTION:

The shift from large centralized energy resources to small battery located at the point of consumption is one of the emerging trends in the electricity industry with having the multiple advantages over the traditional energy technologies, like improved asset utilization, better power quality, and enhanced power system reliability and capacity. The renewable energy sources, like solar cells and fuel cells, usually generate dc power. The application of the inverters for the grid inter-connection has become much more popular because of increasing use of the renewable energy resources, mostly the solar PV cells and fuel cells as the battery. A two-stage fuel cell power conditioning

system to deliver AC power has been commonly considered and studied in many technical papers [2], [3], [8]-[14]. The system usually includes transformer type DC-DC boost converter stage and DC to AC inverter stage with auxiliary energy unit in Fig. 1 [8], [13], [14]. This type of power conditioning system has inevitable drawbacks such as being bulky, costly and inefficient because it actually has three power conversion stages (DC to high-frequency AC, then DC and low frequency AC) [3]. In order to minimize the problems with a two-stage fuel cell power conditioning system, a topology with reduced power processing and conversion stages is required. A topology that is suitable for AC loads and is powered from DC sources able to boost and invert the voltage at the same time has been proposed in [13]. The double loop control scheme of this topology has also been proposed for better performance even during transient conditions [14].

However, if such topology was to be used for an AC load to be powered by an FC, the FC would be exposed to a number of problems such as load variation, slow respond and current ripple. In this case, an energy storage back-up unit would be required to address the previously mentioned problems. The objective of this paper is to propose and report full simulation results of a grid-connected single-phase FC system using a single energy conversion stage only. In particular, the proposed system, based on the boost inverter with a battery storage unit, solves the previously mentioned issues (e.g., the low and variable output voltage of the FC, its slow dynamics, and current harmonics on the FC side). The single energy conversion stage includes both boosting and inversion functions and provides high power conversion efficiency, reduced converter size, and low cost. The proposed single phase grid-connected FC system can operate either in grid connected or stand-alone mode. In the grid-connected mode, the boost inverter is able to control the active (P) and reactive (Q) powers through the grid by the proposed PQ control algorithm using fast signal conditioning for single-phase systems.

II. PROPOSED FC ENERGY SYSTEM:

The proposed three-phase FC stand-alone power supply consists of two power converters: the three-phase boost-inverter and the bidirectional back-up unit as shown in Fig.1 also show the laboratory setup for the proposed three-phase FC power supply. The boost-inverter is supplied by the FC and the back-up unit, which are both connected to the same unregulated dc bus while the output side of the converter is connected to a balanced three-phase resistive load. The FC system incorporates a current mode controlled bidirectional converter with battery-based energy storage to support the FC power generation and three voltage-controlled boost converters making up the three-phase boost-inverter stage.

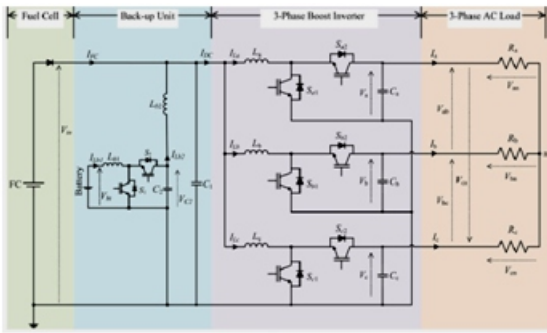


Fig.1.FC sourced stand-alone power supply based on the three-phase boost-inverter.

A. Description of the Three-Phase Boost-Inverter:

The three-phase boost-inverter consists of three identical bidirectional boost converters and their outputs are connected to a three-phase ac load, as shown in Fig.1 The dc-biased three phase output voltages are described by

$$\begin{aligned} V_a &= V_{dc} + A_o \cdot \sin \theta \\ V_b &= V_{dc} + A_o \cdot \sin \left(\theta - \frac{2\pi}{3} \right) \\ V_c &= V_{dc} + A_o \cdot \sin \left(\theta + \frac{2\pi}{3} \right) \end{aligned} \quad (1)$$

Where A_o is the peak amplitude of line-to-neutral voltage and V_{dc} is the dc offset voltage of each boost converter and has to be greater than $A_o + V_{in}$. Each boost converter generates a dc bias with deliberate ac output voltage (a dc-biased sinusoidal waveform as an output), so that the individual boost converters generate a unipolar voltage greater than the FC output voltage with a variable duty cycle.

The dc components are canceled in the three-phase three-wire balanced output and the line-to-line voltages are described by

$$\begin{aligned} V_{ab} &= V_a - V_b = \sqrt{3}A_o \cdot \sin \left(\theta + \frac{\pi}{6} \right) \\ V_{bc} &= V_b - V_c = \sqrt{3}A_o \cdot \sin \left(\theta + \frac{5\pi}{12} \right) \\ V_{ca} &= V_c - V_a = \sqrt{3}A_o \cdot \sin \left(\theta - \frac{5\pi}{12} \right) \end{aligned} \quad (2)$$

From (2), it can be noticed that the line-to-line voltages contain only the ac component. This concept was first discussed. When the three-phase outputs are balanced and node "n" is floating as shown, the line-to-neutral voltages in the load side do not include any dc component as described by

$$\begin{aligned} V_{an} &= \frac{2}{3}V_a - \frac{1}{3}V_b - \frac{1}{3}V_c = V_a \\ V_{bn} &= \frac{2}{3}V_b - \frac{1}{3}V_a - \frac{1}{3}V_c = V_b \\ V_{cn} &= \frac{2}{3}V_c - \frac{1}{3}V_a - \frac{1}{3}V_c = V_c. \end{aligned} \quad (3)$$

A double-loop control scheme is chosen for the boost-inverter control being the most appropriate method to control the individual boost converters covering the wide range of operating points. Specifically, this control method provides stable operating condition using direct current control of the inductor even in special conditions such as non-linear loads, load variations, and transient short circuits. The boost-inverter is based on the voltage mode control, as shown in Fig.2. The voltages across C_a , C_b , and C_c and the currents through L_a , L_b , and L_c are controlled by proportional-integral (PI) controllers, which have been tuned to achieve good performance and stability margins. The model equations based on the averaging concept for each boost converter are expressed by

$$v_{in} - v_{Lx} = (1 - d_x) \cdot v_x \quad (4)$$

$$i_{cx} - i_x = (1 - d_x) \cdot i_{Lx} \quad (5)$$

Where x represents each phase (a,b, and c), v_{Lx} and i_{Lx} are the inductor voltage and current, v_x and $i_c x$ are the capacitor voltage and current, i_x is the output phase current, and d_x is the duty cycle. When the internal resistances of the inductors and capacitors are ignored, the differential equations of the inductor voltage and capacitor current are expressed by

$$v_{Lx} = L_x \cdot \frac{d \cdot i_{Lx}}{dt} \quad (6)$$

$$i_{Cx} = C_x \cdot \frac{d \cdot v_x}{dt} \quad (7)$$

where L_x and C_x are inductance and capacitance. In the double-loop control scheme, inductor voltages and capacitor currents are used as control variables for the current and voltage control loops. The duty cycles need to remain between 0.15 and 0.85 p.u. to generate sinusoidal output voltage. Based on the averaging concept and the continuous conduction mode (CCM) for the boost converter, the duty cycles can be expressed by using (4)

$$d_x = 1 - \frac{v_{in} - v_{Lx.ref}}{v_x} \quad (8)$$

Where $v_{Lx.ref}$ is the inductor voltage reference as control variable for the current control loop. The V_x and V_{in} in (8) provide a compensation of the variable gain of the boost converters and cancelation of the input voltage variation.

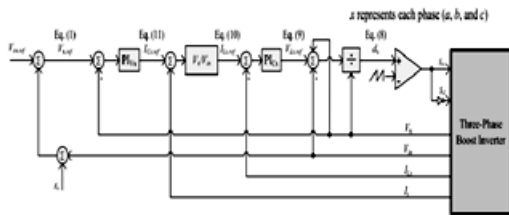


Fig.2. Control block diagram of the three-phase three-line boost-inverter.

The control variable of the inductor voltage reference ($v_{Lx.ref}$) can be obtained by using a PI controller with a current error as follows:

$$v_{Lx.ref} = \left(K_{PCx} + \frac{1}{K_{ICx} \cdot s} \right) \cdot (i_{Lx.ref} - i_{Lx}) \quad (9)$$

Where K_{PCx} and K_{ICx} are the proportional gain and integral gain for the inner current control loop.

From (5) and (8), if the inductor energy variations are ignored the inductor current reference ($i_{Lx.ref}$) of the current controller is given by

$$i_{Lx.ref} = \frac{v_x}{v_{in}} \cdot (i_{cx.ref} + i_x), \text{ when } v_{Lx.ref} \approx 0 \quad (10)$$

Where $i_{Cx.ref}$ is the capacitor current reference as control variable for the voltage control loop.

The control variable of the capacitor voltage reference ($v_{Cx.ref}$) can be obtained by using a PI controller with a voltage error as follows:

$$i_{Cx.ref} = \left(K_{PVx} + \frac{1}{K_{IVx} \cdot s} \right) \cdot (v_{x.ref} - v_x) \quad (11)$$

where $v_{x.ref}$ is the output voltage references of the three-phase boost-inverter as (1) and K_{PVx} and K_{IVx} are the proportional gain and integral gain for the outer output voltage control loop respectively that should be selected as lower bandwidth compared with the inner loop. Fig. 2 shows the control block diagram of the three-phase three-line boost-inverter including the voltage and current control loops. The dc offset voltage (V_{dc}) is added to the three individual phase voltage references. The dc offset can be obtained by adding the input voltage (V_{in}) to the peak output amplitude (A_o). The V_{dc} can be minimized in order to reduce the output peak voltages of each boost converter and the switching losses in the case of a variable input voltage.

The voltage references ($V_{a.ref}$, $V_{b.ref}$, and $V_{c.ref}$) are compared with the feedback voltages (V_a , V_b , and V_c) of the individual boost converters to generate voltage errors. These voltage errors are processed by PIV_x to generate capacitor current reference as shown in (11). When the capacitor current references and the output current are applied with the block (V_x/V_{in}) each reference current of the inductors are given by (10). These inductor current references are compared with the feedback currents of the inductors (L_x) to produce the current errors. Then, the inductor voltage references expressed in (9) are provided using $PI C_x$ with the current errors. Finally, using (9) the duty cycles can be obtained for the three-phase boost-inverter.

B. Battery Storage Back-Up Unit:

The battery storage back-up unit is designed to support the slow dynamics of the FC [1], [3], [6], [7] and is shown in Fig.1. The back-up unit comprises of a current-controlled 1 kW IGBT-based bidirectional boost converter operating at 20 kHz and the energy storage component. For instance, when a load is connected or disconnected the back-up unit immediately discharge or charge the battery through the bidirectional converter with a limitation of 4 A/s current slew rate. Two generic 12 V–24 Ah lead acid batteries are used for energy storage to deal with the need to provide fast response and a relatively low cost solution. The back-up unit performs not only the support function for the FC module during transients but also recovers any surplus power delivered by the FC. Other energy storage technologies such as lithium-ion batteries or super capacitors can also be used instead of lead-acid but it is beyond the scope of this paper to deal with the type of the storage of the back-up unit.

Additionally, in order to protect the FC system, the back-up unit provides low-frequency ac current harmonics and high frequency switching ripple that is required from the dc-ac boost inverter operation. More detailed analysis of the backup unit based on equivalent circuit of the PEMFC has been presented. The paper illustrates the compensation characteristics for the low-frequency ac ripple using current control and the high frequency ripple performed by LC passive filter. Specifically, C2 and Lb2 are tuned at switching frequency to suppress on the FC side. The duty cycle for the back-up unit based on the averaging concept can be expressed by using

$$d_{BU} = 1 - \frac{v_{bt} - v_{Lb1.ref}}{v_{in}} \quad (12)$$

Where the d_{BU} is the duty cycle, v_{bt} is the battery voltage, and $v_{Lb1.ref}$ is the inductor voltage reference as control variable for the current control loop. The control variable of the inductor voltage reference ($v_{Lb1.ref}$) can be expressed using a PI controller with current error as follows:

$$v_{Lb1.ref} = \left(K_{PBU} + \frac{1}{K_{IBU} \cdot s} \right) \cdot (i_{Lb1.ref} - i_{Lb1}) \quad (13)$$

where K_{PBU} and K_{IBU} are the proportional gain and integral gain for the current controller of the back-up unit. The current reference ($i_{Lb1.ref}$) is determined by I_{dc} through a high-pass

filter (HPF) and the demanded current (I_{demand}) that is related to the load change. In order to detect the ac components higher than the fundamental frequency, a relatively low cut-off frequency has been used as 5 Hz. The ac component of the current reference deals with the elimination of the ac ripple current from the FC power module while the dc component deals with the slow dynamics of the FC.

C. Design Guidelines:

The design parameters are given in Table I. The following equations have been used in order to calculate the inductor and capacitor values

$$i_L(\max) = \frac{V_{in} - \sqrt{V_{in}^2 - 4R_a(-V_{\max}(t)) \cdot ((V_{\min}(t) - V_{\max}(t))/R_{eq})}}{2R_a} \quad (14)$$

$$\Delta i_L(t) = \frac{(V_{in} - R_a i_L(t)) \cdot \Delta t_1}{L} \quad (15)$$

where $i_L(\max)$ is maximum inductor current and Δi_L is high frequency ripple current of the inductor caused by the switching operation. In (14), the single-phase model equivalent resistance (R_{eq}) can be introduced

$$R_{eq} = \frac{3}{2} R_a \quad (16)$$

The maximum inductor current ripple Δi_{Lmax} is chosen to be equal to 5% of the maximum inductor current, as calculated from (14). From (14) and (15), the inductance is calculated and chosen as 700 μ H for L_a, L_b , and L_c . The ripple voltage of the C_1 and C_2 is given by

$$\Delta V_c = \left(\frac{V_{\min}(t) - V_{\max}(t)}{C_x \cdot R_{eq}} \right) \cdot \Delta t_1 \quad (17)$$

From (17), a capacitor value has been obtained as 12 μ F and a 20 μ F 800 V rated metalized polypropylene film capacitor has been used for C_a, C_b , and C_c for the experimental prototype. The design parameters of the backup unit have been obtained as 150 μ H and 20 μ F using (15) and (17).

III. MATLAB/SIMULINK RESULTS:

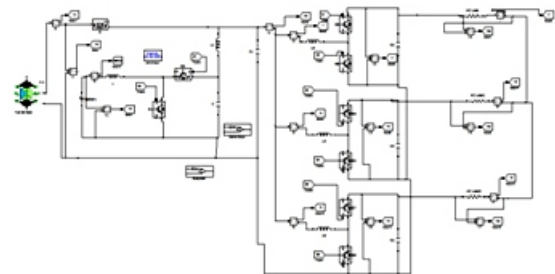


Fig.3. Matlab/Simulink model of FC sourced stand-alone power supply based on the three-phase boost inverter.

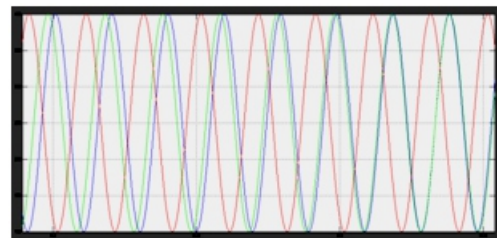


Fig.4. Simulation results of the proposed FC stand-alone power supply Output voltages of each boost converter.

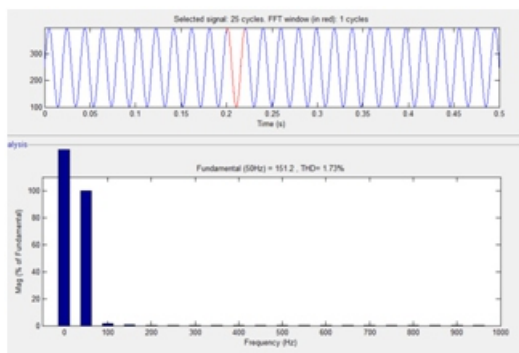


Fig.5. FFT result for the output voltages.

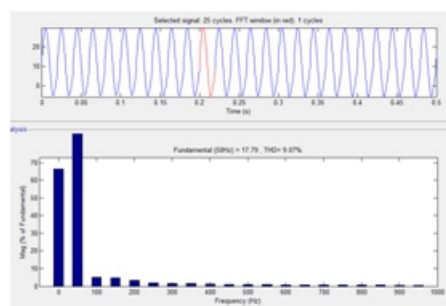


Fig.10. FFT results for the inductor currents.

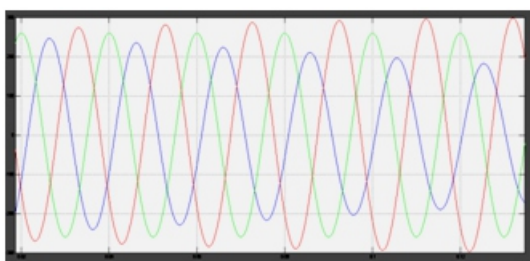


Fig.6. Line-to-line output voltages of the boost-inverter.



Fig.11. Duty cycles of the boost-inverter, d_a , d_b , and d_c .

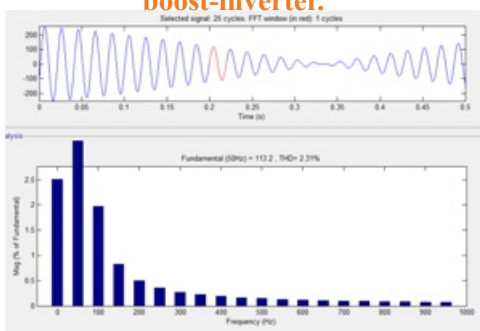


Fig.7. FFT result for the line-to-line outputs.



Fig.12. Simulation results of the proposed FC stand-alone power supply Input current of the boost-inverter, I_{DC} .

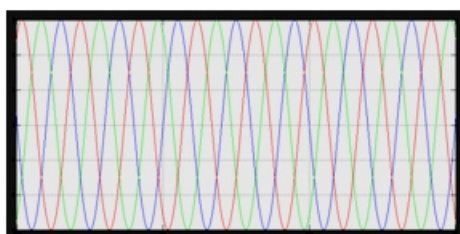


Fig.8. Three-phase load currents.

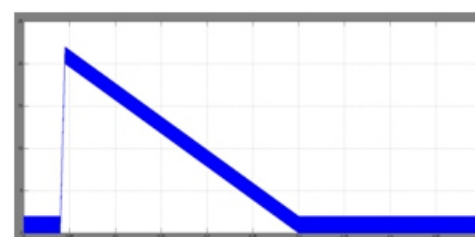


Fig.13. Output current of the back-up unit, I_{Lb2} .

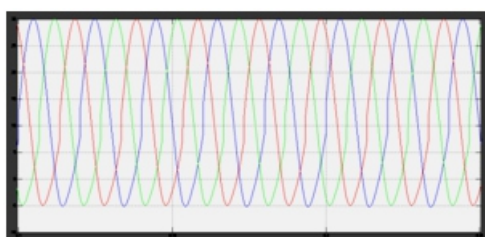


Fig.9. Inductor currents through L_a , L_b , and L_c .

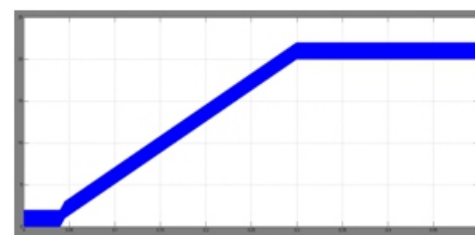


Fig.14. FC output current during transient, I_{FC} .

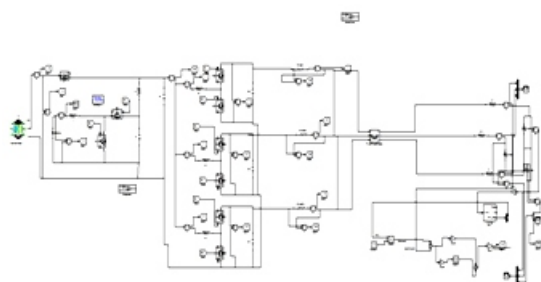


Fig.15.matlab/simulink model of FC sourced stand-alone power supply based on the three-phase boost-inverter with grid connected system.

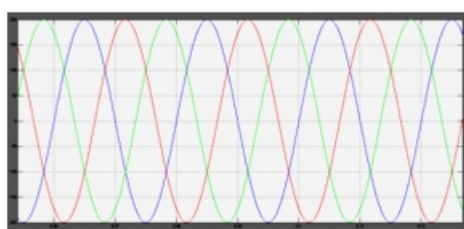


Fig.16.grid voltage.

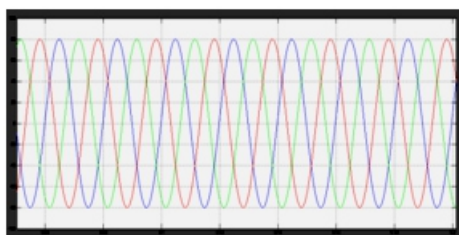


Fig.17.grid current.

IV.CONCLUSION:

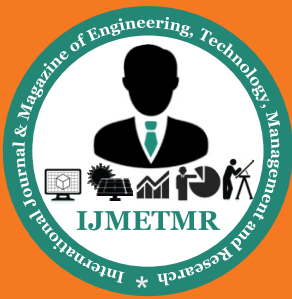
A stand-alone three-phase FC sourced power supply based on the boost-inverter topology with a back-up battery-based energy storage unit has been proposed in this paper. The presented simulation results have verified the operation characteristics of the power supply.

The results of the proposed three-phase FC supply have confirmed its satisfactory performance in delivering boosting and inversion functions in one conversion stage to generate 210 Vac from 43 Vdc at rated power.

The back-up unit key function is to support the slow dynamics of the FC. The presented simulation results have verified the operation characteristics of the power supply with grid connected simulated to the grid voltage and current.

REFERENCES:

- [1] M. E. Schenck, J.-S. Lai, and K. Stanton, "Fuel cell and power conditioning system interactions," in Proc. IEEE Appl. Power Electron. Conf. Expo., 2005, vol. 1, pp. 114–120.
- [2] M. W. Ellis, M. R. Von Spakovsky, and D. J. Nelson, "Fuel cell systems: Efficient, flexible energy conversion for the 21st century," Proc. IEEE, vol. 89, no. 12, pp. 1808–1818, Dec. 2001.
- [3] J.-S. Lai, "Power conditioning circuit topologies," IEEE Ind. Electron. Mag., vol. 3, no. 2, pp. 24–34, Jun. 2009.
- [4] Horizon Fuel Cell Technologies. H-Series PEMFC system user guide (2010). [Online]. Available: <http://www.horizonfuelcell.com>
- [5] J. M. Correa, F. A. Farret, J. R. Gomes, and M. G. Simoes, "Simulation of fuel-cell stacks using a computer-controlled power rectifier with the purposes of actual high-power injection applications," IEEE Trans. Ind. Appl., vol. 39, no. 4, pp. 1136–1142, Jul./Aug. 2003.
- [6] J. Lee, J. Jo, S. Choi, and S.-B. Han, "A 10-kW SOFC low-voltage battery hybrid power conditioning system for residential use," IEEE Trans. Energy Convers., vol. 21, no. 2, pp. 575–585, Jun. 2006.
- [7] P. Thounthong, B. Davat, S. Rael, and P. Sethakul, "Fuel cell high-power applications," IEEE Ind. Electron. Mag., vol. 3, no. 1, pp. 32–46, Mar. 2009.
- [8] P. Ching-Tsai and L. Ching-Ming, "A high-efficiency high step-up converter with low switch voltage stress for fuel-cell system applications," IEEE Trans. Ind. Electron., vol. 57, no. 6, pp. 1998–2006, Jun. 2010.
- [9] J. Anzicsek and M. Thompson, "DC–DC boost converter design for Kettering University's GEM fuel cell vehicle," in Proc. Elect. Insul. Conf. Elect. Manuf. Expo, 2005, pp. 307–316.
- [10] K. Jin, X. Ruan, M. Yang, and M. Xu, "Power management for fuel-cell power system cold start," IEEE Trans. Power Electron., vol. 24, no. 10, pp. 2391–2395, Oct. 2009.



singlephase high-step-up ZVT boost converter for fuel-cell microgrid system,” IEEE Trans. Power Electron., vol. 25, no. 12, pp. 3057–3065, Dec. 2010.

[12] J. i. Itoh and F. Hayashi, “Ripple current reduction of a fuel cell for a single-phase isolated converter using a DC active filter with a center tap,” IEEE Trans. Power Electron., vol. 25, no. 3, pp. 550–556, Mar. 2010.

[13] R.-J. Wai and C.-Y. Lin, “Active low-frequency ripple control for clean energy power-conditioning mechanism,” IEEE Trans. Ind. Electron., vol. 57, no. 11, pp. 3780–3792, Nov. 2010.

[14] W. Zhang, D. Xu, X. Li, R. Xie, H. Li, D. Dong, C. Sun, and M. Chen, “Seamless transfer control strategy for fuel cell uninterruptible power supply system,” IEEE Trans. Power Electron., vol. 28, no. 2, pp. 717–729, Feb. 2013.